

1 Dual element (C-Cl) isotope approach to distinguish  
2 abiotic reactions of chlorinated methanes by Fe(0) and by  
3 Fe(II) on iron minerals at neutral and alkaline pH

4  
5 Diana Rodríguez-Fernández<sup>†</sup>, Benjamin Heckel<sup>§</sup>, Clara Torrentó<sup>‡</sup>, Armin Meyer<sup>§</sup>, Martin Elsner<sup>§</sup>, Daniel Hunkeler<sup>‡</sup>,  
6 Albert Soler<sup>†</sup>, Mònica Rosell<sup>†</sup>, Cristina Domènech<sup>†</sup>

7 <sup>†</sup>Grup MAiMA, Mineralogia Aplicada, Geoquímica i Geomicrobiologia, Departament de Mineralogia, Petrologia i  
8 Geologia Aplicada, Facultat de Ciències de la Terra, Martí Franquès s/n, Universitat de Barcelona (UB), 08028  
9 Barcelona, Spain.

10 <sup>§</sup>Institute of Groundwater Ecology, Helmholtz Zentrum München, 85764 Neuherberg, Germany.

11 <sup>‡</sup>Centre d'hydrogéologie et de géothermie, Université de Neuchâtel, Neuchâtel 2000, Switzerland.

12 **Corresponding author:** Diana Rodríguez-Fernández (diana.rodriguez@ub.edu)

13 **Journal:** Chemosphere

14 Figures:4

15 Tables: 2

20 **Abstract**

21  
22 A dual element C-Cl isotopic study was performed for assessing chlorinated methanes (CMs) abiotic  
23 transformation reactions mediated by iron minerals and Fe(0) to further distinguish them in natural  
24 attenuation monitoring or when applying remediation strategies in polluted sites. Isotope fractionation was  
25 investigated during carbon tetrachloride (CT) and chloroform (CF) degradation in anoxic batch experiments  
26 with Fe(0), with FeCl<sub>2</sub>(aq), and with Fe-bearing minerals (magnetite, Mag and pyrite, Py) amended with  
27 FeCl<sub>2</sub>(aq), at two different pH values (7 and 12) representative of field and remediation conditions. At pH  
28 7, only CT batches with Fe(0) and Py underwent degradation and CF accumulation evidenced  
29 hydrogenolysis. With Py, thiolytic reduction was revealed by CS<sub>2</sub> yield and is a likely reason for different  
30  $\Lambda$  value ( $\Delta\delta^{13}\text{C}/\Delta\delta^{37}\text{Cl}$ ) comparing with Fe(0) experiments at pH 7 ( $2.9\pm 0.5$  and  $6.1\pm 0.5$ , respectively). At  
31 pH 12, all CT experiments showed degradation to CF, again with significant differences in  $\Lambda$  values  
32 between Fe(0) ( $5.8\pm 0.4$ ) and Fe-bearing minerals (Mag,  $2\pm 1$ , and Py,  $3.7\pm 0.9$ ), probably evidencing other  
33 parallel pathways (hydrolytic and thiolytic reduction). Variation of pH did not significantly affect the  $\Lambda$   
34 values of CT degradation by Fe(0) nor Py.  
35 CF degradation by Fe(0) at pH 12 showed a  $\Lambda$  ( $8\pm 1$ ) similar to that reported at pH 7 ( $8\pm 2$ ), suggesting CF  
36 hydrogenolysis as the main reaction and that CF alkaline hydrolysis ( $13.0\pm 0.8$ ) was negligible.  
37 Our data establish a base for discerning the predominant or combined pathways of CMs natural attenuation  
38 or for assessing the effectiveness of remediation strategies using recycled minerals or Fe(0).  
39 **keywords (6 words): CSIA, carbon tetrachloride, chloroform, pyrite, Fe(0), degradation pathways**

## 40 1. Introduction

41 Chloroform (CF,  $\text{CHCl}_3$ ) and carbon tetrachloride (CT,  $\text{CCl}_4$ ) are chlorinated volatile organic compounds  
42 (VOCs) from the group of chlorinated methanes (CMs). Both are toxic and predicted to be carcinogenic  
43 substances (IARC, 1999). They are found in groundwater as a consequence of releases from chemical  
44 manufacturing processes or accidental spills (Zogorski et al., 2006), although CF can also be naturally  
45 formed (Cappelletti et al., 2012; Hunkeler et al., 2012; Breider et al., 2013).

46 Abiotic CMs degradation in groundwater mainly proceeds under anoxic conditions. The main CT  
47 degradation pathway is hydrogenolysis to CF, although CT reduction followed by hydrolytic or thiolytic  
48 substitution of dechlorinated intermediates to CO,  $\text{CO}_2$  or  $\text{CS}_2$  is also possible (He et al., 2015). Abiotic CF  
49 degradation processes under anoxic conditions include hydrogenolysis to DCM and reductive elimination  
50 to  $\text{CH}_4$  (Song and Carraway, 2006; He et al., 2015). Bioremediation strategies for CMs are scarce (Penny  
51 et al., 2010; Cappelletti et al., 2012; Koenig et al., 2015). Thus, although both compounds can be biotically  
52 (Penny et al., 2010; Cappelletti et al., 2012) or abiotically degraded, they are considered recalcitrant  
53 compounds requiring targeted remediation strategies in groundwater.

54 *In situ* chemical oxidation is not an effective treatment for CT and CF due to the highly oxidized state of  
55 carbon (Huang et al., 2005; Huling and Pivetz, 2006). Alkaline hydrolysis (AH) has been studied for CF at  
56 laboratory and field scale as a new and effective remediation strategy (Torrentó et al., 2014) but CT  
57 hydrolysis is pH independent and extremely slow (Jeffers et al., 1989). Fortunately, zero-valent metals and  
58 Fe-bearing minerals have proven to mediate the transformation of CF and CT at laboratory scale (e.g.  
59 Matheson and Tratnyek, 1994; Támara and Butler, 2004; Feng and Lim, 2005; Zwank et al., 2005; He et  
60 al., 2015; Lee et al., 2015). Fe(0) has been commonly used in permeable reactive barriers (PRBs) since it  
61 is a strong reducing agent, cheaper and less harmful than other zero-valent metals (Vodyanitskii, 2014).  
62 Micro-sized Fe(0) has been used in long-functioning PRBs, while nano-sized Fe(0) injections have been  
63 recently used to renew PRBs in highly polluted sites (Obiri-Nyarko et al., 2014). Some minerals such as  
64 magnetite ( $\text{Fe}_3\text{O}_4$ , Mag hereafter) can be formed in Fe(0) PRBs reducing their efficiency (Vodyanitskii,  
65 2014), while others, such as FeS, can promote CT degradation (Obiri-Nyarko et al., 2014). Since long-term  
66 evolution of PRBs is still not fully understood (Obiri-Nyarko et al., 2014) and Fe-bearing minerals such as  
67 pyrite ( $\text{FeS}_2$ , Py hereafter), green rusts or Mag are naturally ubiquitous in anoxic aquifers and/or in  
68 transition zones (Ferrey et al., 2004; Scheutz et al., 2011), it is interesting to assess their influence on CMs  
69 degradation.

70 Detection of CMs natural attenuation or monitoring of the above-mentioned remediation strategies can be  
71 challenging when relying on only by-products, since these daughter products can be further degraded, are  
72 difficult to quantify in the field (e.g. gases), could come from other parent compounds or stem from a  
73 secondary source (i.e. CF). In such cases, compound specific isotope analysis (CSIA) has been developed  
74 and matured into a widely applied method allowing the investigation of VOCs transformation reactions and  
75 the associated isotopic fractionation values ( $\epsilon$ ) (Renpenning and Nijenhuis, 2016). The occurrence of  
76 limiting steps prior to the reaction step that mask the real magnitude of the  $\epsilon$  has been shown when mineral  
77 phases are involved in abiotic degradation processes (Elsner et al., 2007). Controlled laboratory studies are  
78 thus required to confine the ranges of possible  $\epsilon$  values and determine conservative estimates of  
79 quantification of CMs degradation extent in the field. The concept of dual element (C-Cl) isotope plots  
80 featuring slopes ( $\Lambda = \Delta\delta^{13}\text{C}/\Delta\delta^{37}\text{Cl}$ ) that are characteristic of different reaction mechanism holds promise to  
81 provide information on the manner and order of chemical bond cleavage for organohalides (Nijenhuis et  
82 al., 2016) and this, in turn, may help to distinguish potential competing processes and to assess their  
83 individual effectiveness as field remediation strategies (Van Breukelen, 2007). Although some abiotic  $\Lambda$   
84 values for CF were recently published (Heckel et al., 2017a; Torrentó et al., 2017), neither  $\Lambda$  for CT abiotic  
85 reactions nor field demonstrations are available.

86 In a multiple-compound polluted site in Òdena (Catalonia) (Palau et al., 2014), shifts in carbon isotopic  
87 composition of CF were attributed to AH (Torrentó et al., 2014) since alkaline conditions (pH ~12) were  
88 generated in recharge water concrete-based interception trenches. In contrast, detected shifts in the carbon  
89 isotopic composition of CT could not be explained by AH but here, reduction by Fe-bearing materials from  
90 the construction wastes used in the trenches could have played an important role (Torrentó et al., 2014).  
91 The presence of surficial iron patinas growths and of variable iron amounts in concrete-based aggregates  
92 obtained from one of the boreholes was confirmed by Scanning Electron Microscopy with X-ray  
93 microanalysis (SEM-EDS) and X-ray fluorescence (XRF) (data not published), but specific mineral phases  
94 are still under study.

95 In order to close this knowledge gap on isotopic data of abiotic CMs reactions and, therefore, to allow better  
96 field interpretations such as in the case of Òdena, this study aims at providing dual element isotope data on  
97 abiotic degradation of CT and CF by Fe(0) and Fe-bearing minerals with  $\text{FeCl}_2(\text{aq})$  under anoxic conditions  
98 at pH 7 and 12. Characterization is based on monitoring the carbon and chloride isotopic composition ( $\delta^{13}\text{C}$   
99 and  $\delta^{37}\text{Cl}$ ) of CF and CT, as well as on detecting volatile dissolved by-products to identify the existence of

100 parallel reaction pathways. Nano-sized Fe(0) was used for CT experiments because it is more reactive than  
101 micro-sized Fe(0) (Song and Carraway, 2006). CF experiments at pH 12 were performed with milli-sized  
102 Fe(0) to compare the pH effect with published pH 7 experiments (Torrentó et al., 2017). Py and Mag were  
103 chosen as Fe-bearing minerals because they involve different potential redox species for reaction with  
104 CMs (Fe(II), and  $S_2^{2-}$  in Py, according to Kriegman-King and Reinhard, 1994) and represent  
105 widespread oxidation products of Fe(0) in PRBs (He et al., 2015) and mining or industrial wastes, which  
106 are potential recyclable materials for remediation.

## 107 **2. Materials and methods**

### 108 **2.1. Experimental setup**

109 Experiments were prepared in an anaerobic chamber and performed in 42 mL VOA/EPA glass vials capped  
110 with PTFE-coated rubber stoppers and plastic screw caps. A summary of experiment nomenclature,  
111 amendments and concentrations, incubation parameters representative of typical environmental conditions  
112 and performed analyses is provided in Table 1, together with data from already published CF experiments  
113 with milli-sized Fe(0) at pH 7 (Torrentó et al., 2017) for the sake of comparison. After the addition of the  
114 solid phase, vials were completely filled with buffered aqueous solution (at pH 7 or 12) without headspace,  
115 except for CT experiments with nano-sized Fe(0), for which the vials contained 21 mL liquid phase and 21  
116 mL gas phase. For Mag and Py batches,  $FeCl_2(aq)$  was also added to the buffered solution to better mimic  
117 field conditions, and because it is thought that CT degradation reactions can be surface-mediated by Fe(II)  
118 sorbed to solid phases (Scherer et al., 1998; Amonette et al., 2000; Pecher et al., 2002; Elsner et al., 2004).  
119 Bottles with 0.6 mM of  $FeCl_2(aq)$  and without Fe-minerals (named as 'aq') were prepared as reactive  
120 controls for the potential of  $FeCl_2(aq)$  for CMs degradation. Controls (CO) with only buffered solution at  
121 the corresponding pH were prepared to observe losses or effects of the pH itself on CF transformation. The  
122 reaction started with the addition of pollutant pure phase to reach the initial theoretical concentration. Vials  
123 were placed in horizontal shakers at room temperature until sampling. Replicates (n vials) were prepared  
124 for each experiment and reaction vials were sacrificed at appropriate time intervals. The CT experiments  
125 with nano-sized Fe(0) were conducted in triplicate and headspace samples were taken from each single vial  
126 at appropriate time intervals. Concentration and C and Cl isotope ratios of parent compounds and potential  
127 by-products were monitored over time. The used analytical methods are included in Table 1.

128 Although Eh could not be monitored, it would be assumed below 0 V, postulated as the boundary for anoxic  
129 conditions (Morris et al., 2003; Hosono et al., 2011). At these Eh conditions, Fe(0) (and Py to a lesser

130 extent) is not stable at pH 7 neither 12 (Fig.S1). Thermodynamically, Fe(0) oxidation should occur and  
131 electron release should be expected. More details about chemicals, minerals and Fe(0) preparation and  
132 characterization, sampling, samples preservation and analytical methods are available in the Supplementary  
133 Information (SI).

Table 1. Summary of performed experiments nomenclature, conditions, procedure and analyses. The equipment used for each analysis is specified. n.u.= not used in the experiment, n.a.=not analyzed.

Pollutant	pH	Name	Pollutant concentration (mM)	Fe(0)/mineral loading (m <sup>2</sup> /L)	FeCl <sub>2</sub> (mM)	n vials	Incubation temperature (°C)	Incubation time (days)	Shaker	By-products analyses	δ <sup>13</sup> C analyses of parent compounds and by-products	δ <sup>37</sup> Cl analyses of parent compounds	Ref.				
CT	7	CT_Fe_7	2.6	28	n.u.	1	25±2	0.1	Horizontal <sup>a</sup> 300 rpm	VOCs HS-GC-qMS-1 <sup>d</sup> as described in Heckel et al. (2017b)	HS-GC-IRMS-2 <sup>d</sup> as described in Cretnik et al. (2013)	HS-GC-IRMS-2 <sup>d</sup> as described in Heckel et al. (2017b)	This study				
	12	CT_Fe_12				1	25±2	0.1	Horizontal <sup>a</sup> 300 rpm								
	7	CT_aq_7	0.3	n.u.	0.6	9	17.4±0.3*	11	Horizontal <sup>b</sup> 100 rpm	VOCs, CS <sub>2</sub> HS-GC-MS <sup>e</sup> as described in Torrentó et al. (2017)	SPME-HS-GC-IRMS-1 <sup>e</sup> as described in Martín-González et al. (2015)	HS-GC-qMS-2 <sup>f</sup> as described in Heckel et al. (2017b)  (n.a. for CT_Mag_7)					
	12	CT_aq_12				11	19.2±0.4*	9									
						5	20±2*	0.9									
	7	CT_Mag_7	0.3	17	0.6	20	15±3*	11									
	12	CT_Mag_12				20	20±2*	9									
	7	CT_Py_7	0.3	59	0.6	20	18.7±0.3*	4									
		19				20±1*	7										
12	CT_Py_12	20				20.2±0.1*	1										
CF	7	CF_CO_7	0.9	n.u.	n.u.	6	25±2	2	Horizontal <sup>c</sup> 200 rpm	VOCs HS-GC-TOF-MS <sup>d</sup> as described in Torrentó et al. (2017)	SPME-HS-GC-IRMS-1 <sup>e</sup> as described in Martín-González et al. (2015)	HS-GC-IRMS-2 <sup>d</sup> as described in Heckel et al. (2017b)	Torrentó et al. (2017)				
	12	CF_CO_12	0.4	n.u.	n.u.	12	25±2	9					This study				
	7	CF_Fe_7	0.9	77	n.u.	20	25±2	2					Torrentó et al. (2017)				
	12	CF_Fe_12	0.4			20	25±2	9									
	7	CF_aq_7	0.4	n.u.	0.6	9	17.4±0.5*	8	Horizontal <sup>b</sup> 100 rpm	VOCs, CS <sub>2</sub> HS-GC-MS <sup>e</sup> as described in Torrentó et al. (2014)	SPME-HS-GC-IRMS-1 <sup>e</sup> as described in Martín-González et al. (2015)	HS-GC-qMS-2 <sup>f</sup> as described in Heckel et al. (2017b)	This study				
	12	CF_aq_12				10	17.2±0.7*	23									
	7	CF_Mag_7	0.4	17	0.6	19	17.0±0.5*	21									
	12	CF_Mag_12				20	17.0±0.6*	23									
	7	CF_Py_7	0.4	59	0.6	19	18±1*	21									
	12	CF_Py_12				20	17.4±0.5*	22									

135 <sup>a</sup>R1000 ROTH; <sup>b</sup>Denlay Instruments LTD n°941157; <sup>c</sup>IKA KS 260 BASIC; <sup>d</sup>in Institute of Groundwater Ecology of Helmholtz Zentrum (München); <sup>e</sup>in Universitat de Barcelona; <sup>f</sup>in Université de Neuchâtel. Equipment  
136 abbreviations correspond to headspace (HS)-gas chromatography (GC)- mass spectrometry (MS); HS-GC coupled to a time-of-flight (TOF) MS; GC quadrupole MS (GC-qMS); GC coupled to a isotope ratio mass  
137 spectrometer (GC-IRMS). \*Spot measurement when sampling.

138 **3. Results and discussion**

139 In the following sections, isotope results for CF and CT degradation by the Fe(0), Mag, Py and FeCl<sub>2</sub>(aq)  
140 are presented (Table 2) and compared with literature data. Concentrations were lower than expected in  
141 some experiments probably due to sorption on non-reactive sites of initial or newly formed solid phases as  
142 observed by other authors (Burriss et al., 1995,1998; Kim and Carraway, 2000; Song and Carraway, 2006).  
143 pH was constant for all experiments (SD<0.5) except for CF\_Mag\_12, CF\_Py\_12, CT\_aq\_7, CT\_Mag\_7  
144 (Fig. S2) where higher fluctuations might be attributable to iron corrosion processes and Fe(OH)<sub>3</sub>(am)  
145 formation.

146



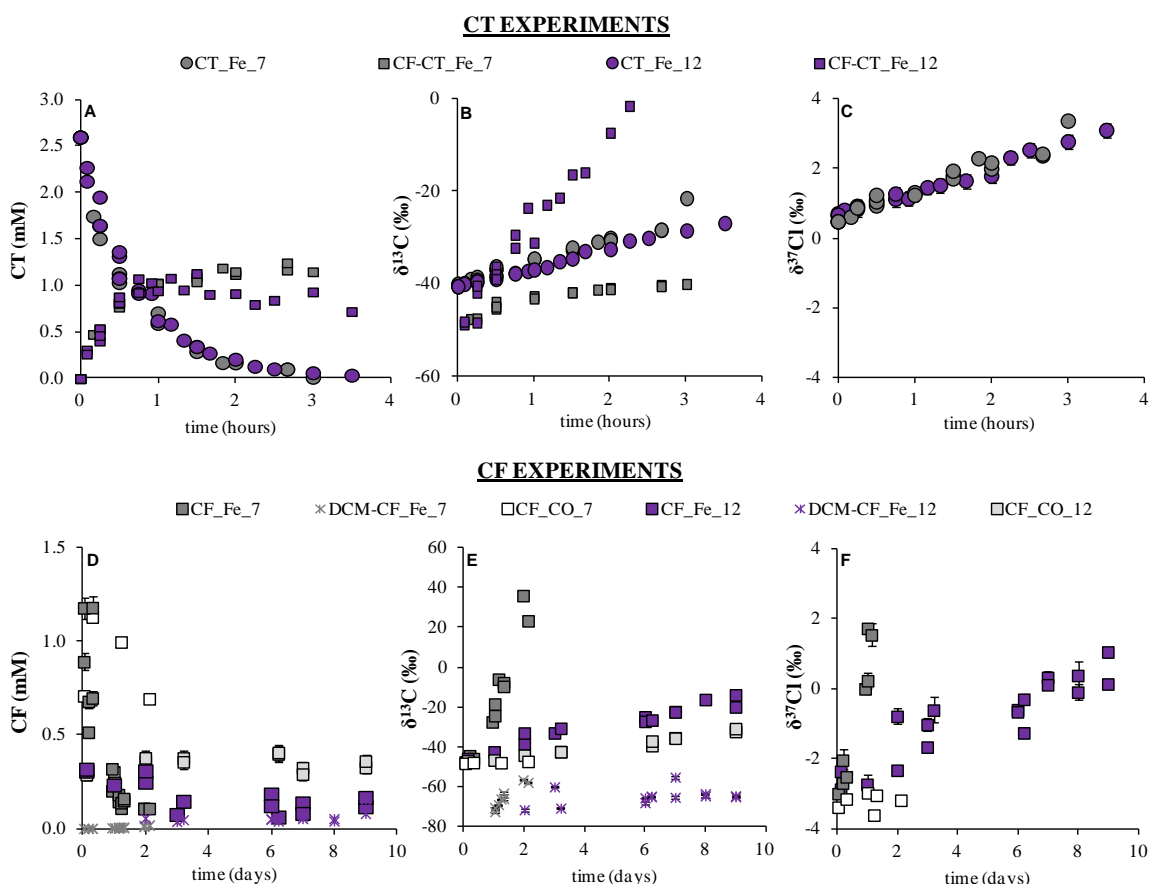
147 Table 2. Summary of isotope results, identified by-products and hypothesized degradation pathways. Uncertainty of  $\epsilon$ , AKIE and  $\Lambda$   
 148 ( $\Delta\delta^{13}\text{C}/\Delta\delta^{37}\text{Cl}$ ) values corresponds to the 95% confidence intervals. AKIEs were calculated assuming C-Cl bond cleavage in the first  
 149 rate-limiting reaction step.  $\text{AKIE}_\text{C}$  values for CT and CF were calculated with  $z=x=n=1$  and  $\text{AKIE}_\text{Cl}$  values with  $z=x=n=4$  for CT and  
 150 of  $z=x=n=3$  for CF (Calculations in SI). Question marks indicate hypothesized pathways not proved in this research.

Experiment	By-products*	$\epsilon$ (%)	AKIE	$\Lambda$	Removal (%)	Proposed pathway
CT_Fe_7	CF	$\epsilon\text{C}=-3.7\pm 0.1$ $R^2=0.995$ $\epsilon\text{Cl}=-0.58\pm 0.04$ $R^2=0.98$	$\text{AKIE}_\text{C}=1.0037\pm 0.0001$ $\text{AKIE}_\text{Cl}=1.00233\pm 0.00004$	$6.1\pm 0.5$ $R^2=0.98$	99	Hydrogenolysis
CT_Fe_12	CF	$\epsilon\text{C}=-3.4\pm 0.1$ $R^2=0.993$ $\epsilon\text{Cl}=-0.55\pm 0.03$ $R^2=0.98$	$\text{AKIE}_\text{C}=1.0034\pm 0.0001$ $\text{AKIE}_\text{Cl}=1.00220\pm 0.00003$	$5.8\pm 0.4$ $R^2=0.98$	99	Hydrogenolysis
CT_aq_7	n.d.	no degradation				
CT_aq_12	CF	$\epsilon\text{C}=-3\pm 3$ $R^2=0.50$	$\text{AKIE}_\text{C}=1.003\pm 0.003$	High confidence interval	87	Hydrogenolysis
CT_Mag_7	n.d.	no degradation				
CT_Mag_12	CF	$\epsilon\text{C}=-2\pm 1$ $R^2=0.70$ $\epsilon\text{Cl}=-0.8\pm 0.2$ $R^2=0.93$	$\text{AKIE}_\text{C}=1.002\pm 0.001$ $\text{AKIE}_\text{Cl}=1.0032\pm 0.0002$	$2\pm 1$ $R^2=0.65$	98	Hydrogenolysis $\pm$ hydrolytic reduction?
CT_Py_7	CF, CS <sub>2</sub>	$\epsilon\text{C}=-5\pm 2$ $R^2=0.70$ $\epsilon\text{Cl}=-1.5\pm 0.4$ $R^2=0.8$	$\text{AKIE}_\text{C}=1.005\pm 0.002$ $\text{AKIE}_\text{Cl}=1.0060\pm 0.0004$	$2.9\pm 0.5$ $R^2=0.9$	99	Hydrogenolysis and thiolytic reduction
CT_Py_12	CF, CS <sub>2</sub>	$\epsilon\text{C}=-4\pm 1$ $R^2=0.87$ $\epsilon\text{Cl}=-0.9\pm 0.4$ $R^2=0.84$	$\text{AKIE}_\text{C}=1.004\pm 0.001$ $\text{AKIE}_\text{Cl}=1.0036\pm 0.0004$	$3.7\pm 0.9$ $R^2=0.93$	99	Hydrogenolysis and thiolytic reduction
CF_CO_7	n.d.	no degradation				
CF_CO_12	n.d.	n.c.	n.c.			Partly by AH $\pm$ reductive elimination?
CF_Fe_7 <sup>a</sup>	DCM	$\epsilon\text{C}=-33\pm 11$ $R^2=0.82$ $\epsilon\text{Cl}=-3\pm 1$ $R^2=0.85$	$\text{AKIE}_\text{C}=1.034\pm 0.012$ $\text{AKIE}_\text{Cl}=1.008\pm 0.001$	$8\pm 2$ $R^2=0.93$	84	Hydrogenolysis $\pm$ reductive elimination?
CF_Fe_12	DCM	$\epsilon\text{C}=-20\pm 9$ $R^2=0.62$ $\epsilon\text{Cl}=-2\pm 1$ $R^2=0.64$	$\text{AKIE}_\text{C}=1.020\pm 0.009$ $\text{AKIE}_\text{Cl}=1.006\pm 0.001$	$8\pm 1$ $R^2=0.92$	85	Hydrogenolysis $\pm$ reductive elimination?
CF_aq_7	n.d.	no degradation				
CF_aq_12	n.d.	$\epsilon\text{C}=-16\pm 13$ $R^2=0.70$	$\text{AKIE}_\text{C}=1.02\pm 0.01$	$\delta^{37}\text{Cl}$ values n.a.	60	Partly by AH $\pm$ reductive elimination?
CF_Mag_7	n.d.	no degradation				
CF_Mag_12	n.d.	$\epsilon\text{C}=-16\pm 9$ $R^2=0.65$	$\text{AKIE}_\text{C}=1.016\pm 0.009$	$\delta^{37}\text{Cl}$ values n.a.	80	Partly by AH $\pm$ reductive elimination?
CF_Py_7	n.d.	no degradation				
CF_Py_12	DCM	$\epsilon\text{C}=-20\pm 7$ $R^2=0.85$	$\text{AKIE}_\text{C}=1.020\pm 0.007$	$\delta^{37}\text{Cl}$ values n.a.	62	Hydrogenolysis $\pm$ reductive elimination and partly by AH?

151 <sup>a</sup>From Torrentó et al. (2017). \*Potential gas by-products such as CO, CO<sub>2</sub>, CH<sub>4</sub> or formate were not analyzed. n.c.= not calculated,  
 152 n.d.=not detected; n.a.=not analyzed  
 153

154 **3.1. Degradation study by Fe(0)**

155 At both pH 7 and 12, CT concentration decrease below the detection limit in experiments with nano-sized  
 156 Fe(0) was achieved before 4h (Fig. 1A) and followed a pseudo-first-order kinetic law with rate constant  
 157 values  $k_{SA}$  of  $(4.9\pm 0.6)\times 10^{-2}$  and  $(4.4\pm 0.1)\times 10^{-2}$  Lm<sup>-2</sup>h<sup>-1</sup>, respectively (Table S1). pH effect on  $k_{SA}$  was  
 158 minimal as expected by thermodynamics, since E<sup>0</sup> of Fe(0) transformation to Fe(II) does not depend on pH.



159  
 160 Fig. 1. Concentration (A, D), carbon (B, E) and chlorine (C, F) isotope composition ( $\delta^{13}\text{C}$  and  $\delta^{37}\text{Cl}$ , ‰) over time in the CT (upper  
 161 panels) and CF (lower panels) experiments at pH 7 and 12 with Fe(0) and control CF experiments (CO). CF\_Fe\_7 and CF\_CO\_7 data  
 162 from Torrentó et al. (2017), and concentration and  $\delta^{13}\text{C}$  evolution of CF and DCM as CT and CF by-products, respectively, are also  
 163 shown.  $\delta^{37}\text{Cl}$  data of by-products are not available. Error bars are smaller than symbols.

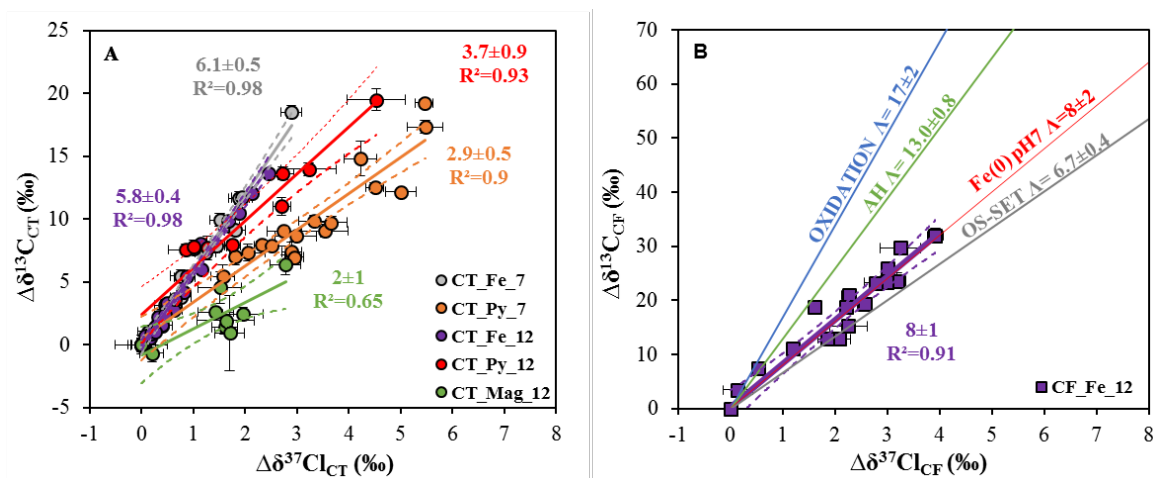
164  
 165 Significant shifts in  $\delta^{13}\text{C}_{\text{CT}}$  and  $\delta^{37}\text{Cl}_{\text{CT}}$  were detected after 99.4% and 98.6% of CT removal at pH 7 and  
 166 12, respectively (Fig. 1B and C), resulting in very similar  $\epsilon_{\text{C}_{\text{CT}}}$  ( $-3.7\pm 0.1$ ,  $R^2=0.995$  and  $-3.4\pm 0.1$ ,  $R^2=0.993$ ,  
 167 respectively, see Eq. S4 and Fig. S3) and  $\epsilon_{\text{Cl}_{\text{CT}}}$  values ( $-0.58\pm 0.04$ ,  $R^2=0.98$  and  $-0.55\pm 0.03$ ,  $R^2=0.98$ ,  
 168 respectively). Calculated AKIE<sub>C</sub> values (Eq. S5) were therefore also similar at pH 7 ( $1.0037\pm 0.0001$ ) and  
 169 12 ( $1.0034\pm 0.0001$ ) as for AKIE<sub>Cl</sub> values ( $1.0023\pm 0.0004$  and  $1.00220\pm 0.00003$ , respectively) (Table S2).  
 170 These similarities regardless of pH confirmed that pH affects primarily intermediate [ $\cdot\text{CCl}_3$ ] radical

171 reactions rather than the initial rate-limiting step (Zwank et al., 2005). AKIEs values were below 50% of  
172 the Streitwieser limit for a C-Cl bond cleavage ( $KIE_C=1.057$ ,  $KIE_{Cl}=1.013$ ) (Elsner et al., 2005) and also  
173 below all reported values for abiotic and biotic reductive dechlorination of chlorinated compounds (Table  
174 S2), indicating significant mass transfer masking effects. CT is rapidly reduced when contacting a strong  
175 reducing agent like Fe(0) and, thus, the rate-limiting step of the reaction might be the diffusion of CT  
176 through the solution to the Fe(0) surface rather than the C-Cl bond cleavage (Arnold et al., 1999). In our  
177 experiments, this diffusion control could have been enhanced by the low concentration of CT (2.6 mM)  
178 compared to Fe(0) loading (28 m<sup>2</sup>/L), but further research would be needed to confirm this hypothesis.

179 The use of HEPES in the pH 7 experiments might constrain exact quantitative by-product distribution as it  
180 appears to alter by-product formation acting as possible H• radical donor and favoring CF formation (Elsner  
181 et al., 2004; Danielsen et al., 2005). However, by-product distribution study was not the aim of this work  
182 and by-products different from VOCs such as CH<sub>4</sub>, CO, CO<sub>2</sub>, (Lien and Zhang, 1999; Choe et al., 2001;  
183 Song and Carraway, 2006) were not analyzed. CF (45-56%) and DCM (up to 0.3% of initial CT) were  
184 detected as by-products at pH 7 and 12, after 99% of CT degradation, similarly to what was reported  
185 previously (Helland et al., 1995; Támara and Butler, 2004; Song and Carraway, 2006; Lien et al., 2007;  
186 Feng et al., 2008), which confirms CT and CF hydrogenolysis. Isotopic mass balances showed a maximum  
187  $\Delta\delta^{13}C_{SUM}$  (defined as final  $\delta^{13}C_{SUM}$ , Eq. S6, with respect to initial  $\delta^{13}C_{SUM}$  considering, CT and by-product  
188 CF data) of only +1.5‰ at pH 7, compared to +35‰ at pH 12. Thus, at pH 7, CF degradation to other by-  
189 product different from DCM was insignificant in the present experimental conditions and duration (3.5  
190 hours). At pH 12, however, important further CF degradation (and a possible formation of other CT by-  
191 products) was evidenced by  $\Delta\delta^{13}C_{SUM}$ ,  $\Delta\delta^{13}C$  and more enriched  $\delta^{13}C_{CF}$  values than those  $\delta^{13}C_{CT}$  values of  
192 the parental CT (Fig. 1B).

193 As carbon and chlorine CT isotope fractionation is affected to the same extent by the above-mentioned  
194 masking effects, in a C-Cl dual plot these effects cancel out. As shown in Fig. 2A,  $\Lambda$  values obtained at pH  
195 7 and 12 are similar ( $6.1\pm 0.5$ ,  $R^2=0.98$  and  $5.8\pm 0.4$ ,  $R^2=0.98$ , respectively), and indicative of CT  
196 hydrogenolysis attending to CF formation. The above-mentioned closed mass balances in CT\_Fe\_7 and the  
197 similar  $\Lambda$  at both pH revealed that CT hydrogenolysis by Fe(0) might also be the main pathway at pH 12.  
198 Moreover, if CT parallel pathways occur at pH 12, they should involve one C-Cl bond cleavage as  
199 hydrogenolysis does (Scheme S1). The obtained  $\Lambda$  values for CT degradation by Fe(0) show no statistically  
200 significant difference (with statistical significance at the  $p<0.05$  level, ANCOVA,  $p=0.8$ ) to that reported

201 for biotically-mediated CT anaerobic degradation detected in field-derived microcosms ( $6.1 \pm 0.5$ )  
 202 (Rodríguez-Fernández et al., 2018).



203

204 Fig. 2. Dual C-Cl isotope plot for CT (A) and CF (B) abiotic experiments. Same coloured solid and dashed lines correspond to linear  
 205 regressions of the data sets of this study and 95% CI, respectively. Error bars show uncertainty in duplicate isotope measurements  
 206 except for CT\_Fe\_7 and CT\_Fe\_12 experiments, where 0.5‰ and 0.2‰ were considered for  $\delta^{13}\text{C}$  and  $\delta^{37}\text{Cl}$ , respectively. In some  
 207 cases, error bars are smaller than symbols. Solid slopes in B correspond to CF abiotic degradation reference systems: oxidation by  
 208 thermally-activated persulfate (blue), alkaline hydrolysis, AH (green), dechlorination by Fe(0) at pH 7 (red) (Torrentó et al., 2017)  
 209 and reductive outer-sphere electron transfer by  $\text{CO}_2$  radical anions, OS-SET (grey) (Heckel et al., 2017a).

210

211 The CF\_Fe\_12 experiments were carried out to complement existing data at pH 7 with milli-sized Fe(0)  
 212 (Torrentó et al., 2017) (CF\_Fe\_7 in Table 1) and to provide, thereby, a more comprehensive picture of  
 213 isotope effects in CF reduction by Fe(0). The corresponding control experiment without Fe(0) (CF\_CO\_12)  
 214 showed certain variation in CF concentration (Fig. 1D) and although no VOCs by-products were detected,  
 215 a significant  $\delta^{13}\text{C}_{\text{CF}}$  shift of +17.6‰ was shown after 9 days (Fig. 1E). Since no isotopic changes occurred  
 216 in previously reported CF\_CO\_7 (Torrentó et al. 2017), the results of CF\_CO\_12 experiment suggest that  
 217 CF was degraded by AH. Assuming this was the only degradation fractionation process, the CF  
 218 transformation extent by AH in CF\_CO\_12 was estimated to be  $27 \pm 7\%$  using Eq. S7 and the  $\epsilon_{\text{C}}$  of  $-57 \pm 5$   
 219 ‰ obtained by Torrentó et al. (2017). This extent of degradation fits well with the reported CF hydrolysis  
 220 rates (Torrentó et al., 2014; 2017).

221 In the CF\_Fe\_12 experiment, CF degradation was also evidenced. CF concentration decreased with some  
 222 fluctuations (Fig. 1D) causing poor correlation in rate constant  $k_{\text{SA}}$  ( $(1.4 \pm 0.6) \times 10^{-3} \text{ Lm}^{-2}\text{d}^{-1}$ ,  $R^2=0.67$ , Table  
 223 S1) and  $\epsilon$  calculations ( $\epsilon_{\text{C}_{\text{CF}}}=-20 \pm 9$ ,  $R^2=0.62$  and  $\epsilon_{\text{Cl}_{\text{CF}}}=-2 \pm 1$ ,  $R^2=0.64$ ) (Fig. S4). Hence, comparison to  
 224 CF\_Fe\_7 and literature data was based on evaluation of  $\Lambda$  values.

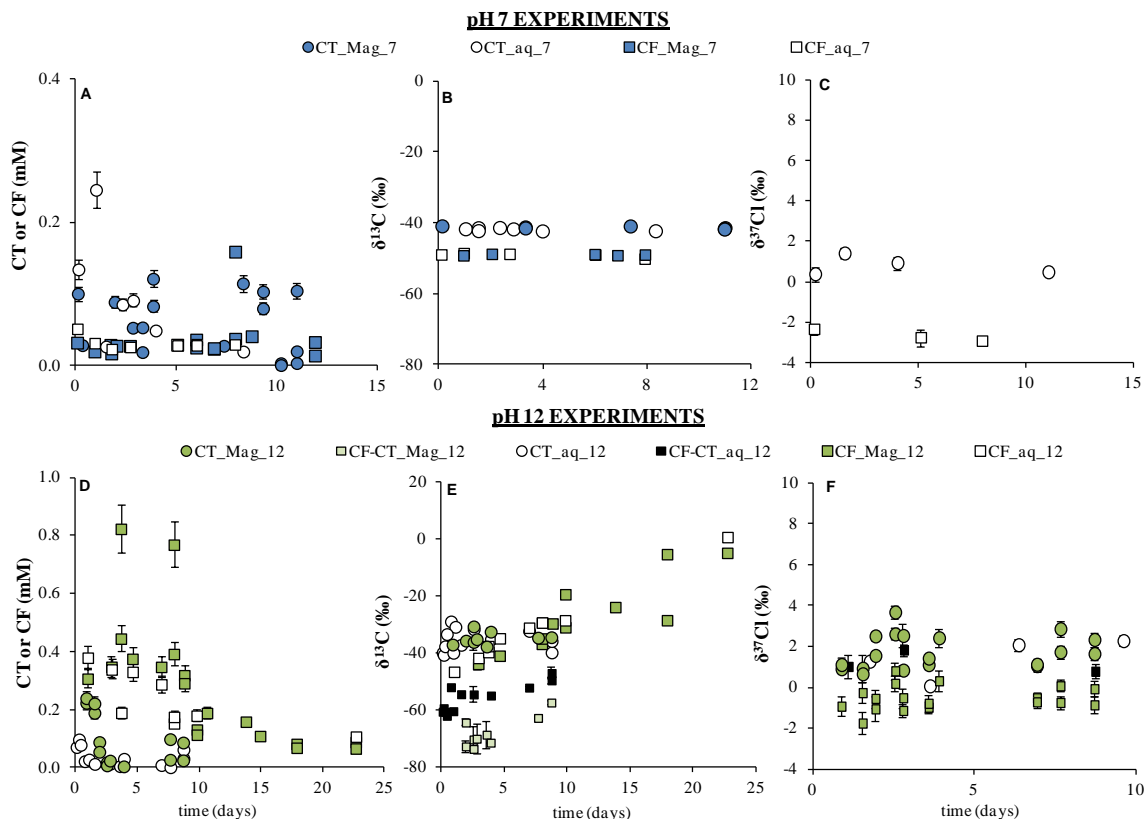
225 In this experiment, a moderated DCM accumulation was detected as by-product ( $\leq 0.3\%$  yield after 9 days).  
226 This, together with the slower CF consumption in CF\_Fe\_12 compared to CF\_Fe\_7 (Fig. 1D), could be  
227 explained by Fe(0) surface passivation due to Fe-oxyhydroxides precipitation, enhanced at alkaline pH  
228 (Farrell et al., 2000; Támara and Butler, 2004). Low  $\Delta\delta^{13}\text{C}_{\text{DCM}}$  was measured at pH 12 (+16‰ after 85%  
229 of CF removal) (Fig. 1E) similar to pH 7 (+15‰, after 87% of CF removal, Torrentó et al., 2017). The  
230  $\Delta\delta^{13}\text{C}_{\text{SUM}}$  (taking into account CF and DCM data) at pH 12 was only around +10‰, which might suggest  
231 an isotope-branching from CF or its intermediates (Zwank et al., 2005), that might have produced the low  
232 DCM carbon isotope fractionation observed for both pH.  
233 The  $\Lambda$  value for CF\_Fe\_12 was  $8 \pm 1$  ( $R^2=0.91$ ), not significantly different from that of Torrentó et al. (2017)  
234 for CF\_Fe\_7 ( $p=0.05065$ ) (Fig. 2B). Combining the data at pH 7 and 12, the  $\Lambda$  value is not significantly  
235 different from that of CF reaction in model systems for outer-sphere single electron transfer (OS-SET) ( $p=$   
236  $0.1056$ ) (Heckel et al., 2017a), suggesting a concerted C-Cl bond cleavage, involving OS-SET in the first  
237 rate-limiting step. For CF\_Fe\_7, Torrentó et al. (2017) postulated two parallel CF dechlorination pathways  
238 (hydrogenolysis and reductive elimination) as reported for other CF reduction studies with micro-sized  
239 Fe(0) (Matheson and Tratnyek, 1994; Feng and Lim, 2005; Song and Carraway, 2006). In the present  
240 experiments, CF reductive elimination related by-products (e.g.  $\text{CH}_4$ , CO and  $\text{HCOO}^-$ ) were not analyzed,  
241 and thus, further conclusions are limited. The similar  $\Lambda$  values for Fe(0) are far from the  $\Lambda=13.0 \pm 0.8$  for  
242 CF AH (Torrentó et al., 2017), indicating that AH in CF\_Fe\_12 was negligible. Accordingly, negligible  
243 contribution of AH was evidenced by assessing the distribution (F) of AH and dechlorination by Fe(0) to  
244 the total CF degradation following Van Breukelen (2007) and using Eq (S8) and  $\epsilon$  data from Torrentó et  
245 al. (2017).

246

### 247 **3.2. Degradation study by FeCl<sub>2</sub>(aq) and Mag**

248 Despite concentration fluctuations (Fig. 3A), no significant  $\delta^{13}\text{C}_{\text{CT}}$  shifts over time were observed in the  
249 CT\_aq\_7 and CT\_Mag\_7 experiments ( $-41.9 \pm 0.5\%$ ,  $n=9$  and  $-41.4 \pm 0.5\%$ ,  $n=6$ , respectively, Fig.3B) and  
250 no VOCs by-products were detected. CT degradation therefore does not seem to occur in these experiments.  
251 In fact, the analogous experiments with CF at pH 7 neither showed also significant changes in  $\delta^{13}\text{C}_{\text{CF}}$  ( $-$   
252  $49.2 \pm 0.2\%$ ,  $n=5$ , and  $-49.0 \pm 0.6\%$ ,  $n=7$ , for CF\_Mag\_7 and CF\_aq\_7 experiments, respectively) (Fig.3B).  
253 This agrees with the decrease in the degradation efficiency of aged Fe(0) PRBs when Mag is formed through  
254 corrosion (Vodyanitskii, 2014). However, CT degradation by Mag has been previously reported in the

255 literature under different experimental conditions (Zwank et al., 2005; Hanoch et al., 2006; Maithreepala  
 256 and Doong, 2007; Vikesland et al., 2007). Further discussion about this discrepancy can be found in the SI.



257

258 Fig. 3. Concentration (A, D) and carbon (B, E) and chlorine (C, F) isotope composition ( $\delta^{13}\text{C}$  and  $\delta^{37}\text{Cl}$ , ‰) over time in the CT and  
 259 CF experiments at pH 7 (upper panels) and 12 (lower panels) with magnetite and  $\text{FeCl}_2(\text{aq})(\text{Mag})$  and  $\text{FeCl}_2(\text{aq})$  alone (aq). Isotope  
 260 data of by-products of each experiment are also shown and named as 'by-product-experiment name' to distinguish them from  
 261 experiments where those compounds are parental compounds. In some cases, error bars are smaller than symbols.

262

263 In contrast, at pH 12, CT degradation occurred and kinetics of CT\_Mag\_12 and CT\_aq\_12 followed a  
 264 pseudo-first-order rate law with a  $k_{SA}$  of  $(8\pm 5)\times 10^{-2}\text{Lm}^{-2}\text{d}^{-1}$  and  $k'$  of  $0.3\pm 0.2\text{d}^{-1}$ , respectively (Table S3).  
 265 CT degradation was confirmed by significant  $\Delta\delta^{13}\text{C}_{\text{CT}}$  (Fig. 3E) and  $\Delta\delta^{37}\text{Cl}_{\text{CT}}$  (Fig. 3F) after 87 and 98%  
 266 CT removal in the CT\_aq\_12 and CT\_Mag\_12 experiments, respectively, obtaining  $\epsilon\text{C}_{\text{CT}} = -2\pm 1\text{‰}$  ( $R^2=0.7$ )  
 267 and  $\epsilon\text{Cl}_{\text{CT}} = -0.8\pm 0.2\text{‰}$  ( $R^2=0.93$ ) for CT\_Mag\_12 (Fig. S6) and  $\epsilon\text{C}_{\text{CT}} = -2\pm 3\text{‰}$  for CT\_aq\_12, but with poor  
 268 linear regression ( $R^2=0.5$ ) (Fig. S7).  $\text{AKIE}_{\text{C}}$  ( $1.002\pm 0.0001$ ) and  $\text{AKIE}_{\text{Cl}}$  ( $1.0032\pm 0.0002$ ) values of  
 269 CT\_Mag\_12 were well below 50% of the Streitwieser limit for a C-Cl bond cleavage (Elsner et al., 2005)  
 270 and also below the reported values for abiotic and biotic reductive dechlorination of chlorinated compounds  
 271 (Table S2), suggesting significant mass transfer masking effects as for Fe(0). A maximum CF yield of  
 272 +38% and +26% in CT\_Mag\_12 and CT\_aq\_12, respectively (Fig. S5), evidenced CT hydrogenolysis.  $\delta^{13}\text{C}$

273 enrichment in the produced CF was detected. To further study CF degradation, analogous experiments with  
274 CF at pH 12 were performed and showed a CF concentration decrease to values down to 0.2-0.1 mM after  
275 23 days (Fig. 3D). Obtained pseudo-first-order rate constants had poor correlation ( $k'=(6\pm 3)\times 10^{-2} \text{ d}^{-1}$ ,  
276  $R^2=0.6$ , for CF\_aq\_12 and  $k_{SA}=(6\pm 2)\times 10^{-3} \text{ Lm}^{-2}\text{d}^{-1}$ ,  $R^2=0.7$ , for CF\_Mag\_12, Table S3). In both experiments  
277 at pH 12, degradation was confirmed by  $\delta^{13}\text{C}$  shifts (Fig.3E). Comparing with the absence of CF  
278 degradation in the pH 7 analogous experiments, AH could be assumed as the main degradation pathway in  
279 these experiments (Torrentó et al., 2017). However, despite poor regression, the obtained values of  $\epsilon_{\text{CF}}$   
280 for CF\_Mag\_12 ( $-16\pm 9\%$ ,  $R^2=0.65$ ) and CF\_aq\_12 ( $-16\pm 13\%$ ,  $R^2=0.70$ ) (Fig. S6, S7) are in the range for  
281 CF reductive dechlorination studies (Table S2) and far away from the reported values for CF AH at pH 12  
282 ( $-57\pm 5\%$ ) (Torrentó et al., 2017). These results suggest the occurrence of additional parallel pathways (such  
283 as CF reductive elimination to  $\text{CH}_4$ ) (Scheme S1). Since nor CF Cl isotope ratios neither other non-  
284 chlorinated potential by-products were measured in these experiments, further conclusions cannot be  
285 drawn.

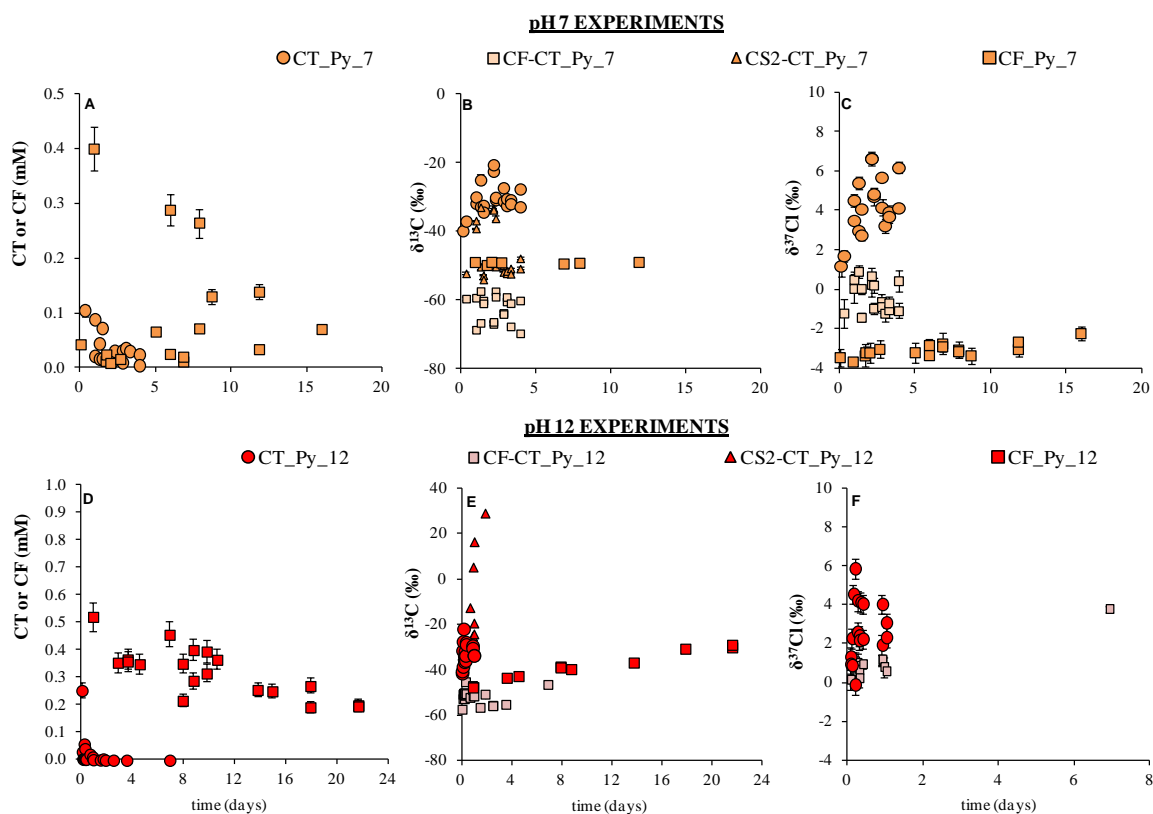
286 The calculated  $\Lambda$  value for CT\_aq\_12 ( $2\pm 3$ ,  $R^2=0.67$ ) was discarded due to its wide confidence interval,  
287 while that for CT\_Mag\_12 ( $2\pm 1$ ,  $R^2=0.65$ ) (Fig. 2A) was, despite its poor linear regression, highly  
288 statistically different ( $p<0.0001$ ) from those of CT\_Fe\_7 and CT\_Fe\_12. It suggests that although CF was  
289 formed as by-product in both Fe(0) and Mag CT experiments, parallel pathways other than hydrogenolysis  
290 could have occurred in CT\_Mag\_12. Also, a different first rate-determining step between reactions such as  
291 that producing CF or CO (hypothesized by-product by CT hydrolytic reduction according to Danielsen and  
292 Hayes (2004) might have occurred. That case would question whether branching in trichloromethyl free  
293 radical [ $\cdot\text{CCl}_3$ ] or trichlorocarbanion [ $:\text{CCl}_3^-$ ] intermediates (Scheme S1) were responsible for by-products  
294 distribution (Danielsen and Hayes, 2004; Elsner et al., 2004; Zwank et al., 2005) because intermediates  
295 branching alone would have not affected CT isotope fractionation and  $\Lambda$  would have been similar.  
296 Differences in  $\Lambda$  value might be also explained by a change in transition states in mineral surfaces (Elsner  
297 et al., 2004).

298 The absence of CT degradation at pH 7 compared to pH 12, might be attributed to the control that pH exerts  
299 on Mag reactivity (see SI for further discussion). Under our experimental conditions, CT degradation by  
300  $\text{FeCl}_2(\text{aq})$  and Mag was only feasible under alkaline conditions. Although further field research would be  
301 required, Mag might be responsible of  $\delta^{13}\text{C}_{\text{CT}}$  fractionation detected in the alkaline trenches of the Òdena

302 field site (Torrentó et al., 2014) given that Mag is an ubiquitous mineral, commonly present in construction  
 303 wastes.

### 304 3.3. Degradation study by Py

305 CT concentrations in CT\_Py\_7 and CT\_Py\_12 decreased quickly, especially at pH 12 where they reached  
 306 0.01 mM after 4h (Fig. 4A, D). Although poor correlated, degradation followed a pseudo-first-order rate  
 307 law for CT\_Py\_7 ( $k_{SA}=(1.6\pm 0.6)\times 10^{-2}$  Lm<sup>-2</sup>d<sup>-1</sup>, R<sup>2</sup>=0.72) and CT\_Py\_12 ( $(2\pm 1)\times 10^{-2}$  Lm<sup>-2</sup>d<sup>-1</sup>, R<sup>2</sup>=0.6),  
 308 (Table S3). CT degradation was confirmed at both pH by enrichment in <sup>13</sup>C and <sup>37</sup>Cl (Fig. 4). Calculated  
 309  $\epsilon_{CT}$  and  $\epsilon_{Cl_{CT}}$  values were  $-5\pm 2\%$  (R<sup>2</sup>=0.7) and  $-1.5\pm 0.4\%$  (R<sup>2</sup>=0.8), respectively for CT\_Py\_7 (Fig. S8),  
 310 and  $-4\pm 1\%$  (R<sup>2</sup>=0.87) and  $-0.9\pm 0.4\%$  (R<sup>2</sup>=0.84), respectively for CT\_Py\_12 (Fig. S9). Corresponding  
 311 AKIE<sub>C</sub> ( $1.005\pm 0.002$  and  $1.004\pm 0.001$ , respectively) and AKIE<sub>Cl</sub> ( $1.0060\pm 0.0004$  and  
 312  $1.0036\pm 0.0004$ , respectively) indicate significant mass transfer masking effects for the same reasons than  
 313 for Fe(0) and Mag experiments. Poor correlation in CT\_Py\_7 might be linked to the low pH reached  
 314 ( $4.7\pm 1.1$ , Fig. S2) that might have caused changes in Py surface (Bonnissel-Gissinger et al., 1998) affecting  
 315 CT degradation.

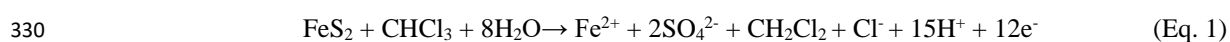


316 Fig. 4. Concentration (A, D) and carbon (B, E) and chlorine (C, F) isotope composition ( $\delta^{13}C$  and  $\delta^{37}Cl$ , ‰) over time in the CT and  
 317 CF experiments at pH 7 (upper panels) and 12 (lower panels) with pyrite (Py) and FeCl<sub>2</sub>(aq). Isotope data of by-products of each  
 318 experiment are also shown and named as 'by-product-experiment name' to distinguish them from experiments where those compounds  
 319 are parental compounds. In some cases, error bars are smaller than symbols.  
 320



321

322 In both experiments, the formation of by-products CF and CS<sub>2</sub> was observed (Fig. S5) agreeing with  
323 literature (Kriegman-King and Reinhard, 1994; Devlin and Muller, 1999). Analogous experiments with Py  
324 and CF as parent compound demonstrated no CF degradation at pH 7 ( $\delta^{13}\text{C}_{\text{CF}}=-49.1\pm 0.3\%$ ,  $\delta^{37}\text{Cl}_{\text{CF}}=-$   
325  $3.1\pm 0.3\%$ ,  $n=7$ ). At pH 12, however, CF degradation was evidenced by a clear CF concentration decrease  
326 ( $k_{\text{SA}}=(2\pm 1)\times 10^{-2}\text{ Lm}^{-2}\text{d}^{-1}$ ,  $R^2=0.6$ ), a significant carbon isotope enrichment ( $\epsilon_{\text{C}_{\text{CF}}}=-20\pm 7\%$ ,  $R^2=0.85$ ) (Fig.  
327 S9) and up to a 6% DCM yield (Fig. S5). Py oxidation at pH 12 by CF is an unknown process but, by  
328 analogy to CT (Kriegman-King and Reinhard, 1992, 1994), it would follow Eq. (1), with an overall reaction  
329 potential higher at pH 12 (0.7 V) than at pH 7 (0.5 V).



331 The accumulation of DCM (Fig. S5) suggests that hydrogenolysis together with AH might be responsible  
332 for CF carbon isotope fractionation. Since  $\delta^{37}\text{Cl}$  was not measured in this experiment, quantification of  
333 each pathway following Eq. (S8) is not possible.

334 The detected CS<sub>2</sub> in the CT experiments with Py (Fig. S5) may form via aqueous or adsorbed HS<sup>-</sup>  
335 (Kriegman-King and Reinhard, 1992) or via S<sub>2</sub><sup>2-</sup> sites on Py surface acting as electron donor (Kriegman-  
336 King and Reinhard, 1994). Despite fluctuations, shifts in  $\delta^{13}\text{C}_{\text{CS}_2}$  values (Fig. 4B) and non-closed isotopic  
337 mass balance calculations at pH 7 ( $\delta^{13}\text{C}_{\text{SUM}}$  range from -44 to -59‰) might reveal further CS<sub>2</sub> degradation  
338 since, as mentioned above, these shifts in  $\delta^{13}\text{C}_{\text{SUM}}$  cannot be attributed to CF degradation. At pH 12, CS<sub>2</sub>  
339 degradation was confirmed by the much enriched  $\delta^{13}\text{C}_{\text{CS}_2}$  values (+28.8‰) with respect to the initial  $\delta^{13}\text{C}_{\text{CT}}$   
340 after 46h (Fig. 4E). CS<sub>2</sub> degradation might occur through hydrolysis mediated by hydroxide ions at these  
341 alkaline conditions ( $11.8 \pm 0.2$ ). CS<sub>2</sub> alkaline hydrolysis has been proven at laboratory scale (Svoronos and  
342 Bruno, 2002) with rate constants at 25 °C ranging between 10<sup>-4</sup> and 10<sup>-3</sup> M<sup>-1</sup>s<sup>-1</sup>, equivalent to half-lives of  
343 1-13 days at pH 11.8. According to literature (Peyton et al., 1976; Adewuyi and Carmichael, 1987;  
344 Kriegman-King and Reinhard, 1992, 1994; McGeough et al., 2007), CS<sub>2</sub> is stable to hydrolysis within the  
345 pH range of 4 to 10, suggesting Py mediation in the potentially occurring CS<sub>2</sub> degradation at pH 7, as Fe(0)  
346 involvement has also been reported (McGeough et al., 2007). Further research is needed to clarify this  
347 point. In any case, it follows that the previously proposed CF:CS<sub>2</sub> mass ratio for distinguishing CT  
348 transformations reactions (Devlin and Muller, 1999; Davis et al., 2003) is inappropriate.

349 The obtained  $\Lambda$  values for CT\_Py\_7 ( $2.9\pm 0.5$ ,  $R^2=0.9$ ) and CT\_Py\_12 experiments ( $3.7\pm 0.9$ ,  $R^2=0.93$ ) are  
350 similar to each other and to that of CT\_Mag\_12 ( $p=0.2302$ ), but they are statistically different from that of

351 CT hydrogenolysis by Fe(0) experiments at both pH values ( $p < 0.0001$ ) (Fig. 2A). CT thiolytic reduction  
352 evidenced by CS<sub>2</sub> formation is thus supported by means of C-Cl  $\Lambda$ . Moreover, since the obtained  $\Lambda$  values  
353 in CT\_Mag\_12 and in CT experiments with Py were similar, a comparable contribution of initial parallel  
354 reaction mechanisms for both reactions is hypothesized (hydrolytic and thiolytic reduction, respectively  
355 Scheme S1).

#### 356 **4. Conclusions**

357 CT and CF degradation by Fe(0) occurs at pH 7 and 12, with similar C-Cl  $\Lambda$  values at both pH values for  
358 each compound ( $8 \pm 2$  and  $8 \pm 1$  for CF;  $6.1 \pm 0.5$  and  $5.8 \pm 0.4$  for CT, respectively), pointing in both cases to  
359 a hydrogenolysis pathway. Accumulation of recalcitrant DCM in this pathway should be taken into  
360 consideration in remediation strategies by PRBs.

361 Isotope fractionation proved that under our experimental conditions, FeCl<sub>2</sub>(aq), Mag and Py are effective  
362 reducing agents for CT at pH 12, whereas at pH 7 only Py was able to degrade CT. CF was detected as by-  
363 product in all CT-degrading experiments, while CS<sub>2</sub> was only detected with Py. The occurrence of parallel  
364 CT hydrogenolysis and hydrolytic or thiolytic reduction pathways was also evidenced by the dual-plot  
365 approach, showing CT experiments with FeCl<sub>2</sub>(aq) and Mag at pH 12 ( $2 \pm 1$ ) and with Py ( $2.9 \pm 0.5$  and  
366  $3.7 \pm 0.9$  at pH 7 and 12)  $\Lambda$  values different than that for hydrogenolysis alone with Fe(0) ( $6.1 \pm 0.5$  at pH 7).  
367 Further CF and CS<sub>2</sub> degradation at pH 12 was confirmed through isotopic tracking, reaffirming that by-  
368 products are not always traceable to confirm parent compound degradation. Mag and Py are thus effective  
369 minerals for abiotic CT remediation strategies, especially under alkaline conditions, where the  
370 accumulation of harmful by-products is avoided by further degradation. On the contrary, under aquifer  
371 conditions, recycling these minerals for cost-effective PRB-building requires ensuring subsequent CF and  
372 CS<sub>2</sub> elimination. The studied CMs degradation reactions might be diffusion-controlled under natural field  
373 conditions, as it was previously reported (Elsner et al., 2007; Thullner et al., 2013). Thus, due to this isotope  
374 masking by rate-limitations in mass transfer, the highest reported  $\epsilon$  value should be used for a conservative  
375 assessment of CMs degradation extent (Elsner et al., 2010; Thullner et al., 2012). However, if these minerals  
376 or Fe(0) were used as remediation techniques, where a high contaminant/mineral ratio is normally used, the  
377 C-Cl bond cleavage might be the rate-limiting step. Nevertheless, further research would be needed to  
378 confirm this hypothesis.

379 To sum up, all the data provided in this dual element C-Cl isotopic approach – especially first-time-  
380 published abiotic CT  $\Lambda$  values – in combination with earlier data for CF abiotic (Heckel et al., 2017a;

381 Torrentó et al., 2017) and CT and CF biotic transformation reactions (Rodríguez-Fernández et al., 2018),  
382 improve considerably the isotopic database of CMs reactions. This information could be further applied in  
383 field studies for discerning the predominant pathway or the contribution of combined pathways in CMs  
384 natural attenuation following Van Breukelen (2007) or assessing the effect of remediation treatments over  
385 time.

## 386 **Appendix A. Supplementary data**

387 Supplementary data to this article can be found online at:

## 388 **Acknowledgements**

389 This research was supported by a Marie Curie Career Integration Grant in the framework of IMOTEC-  
390 BOX project (PCIG9-GA-2011-293808), the Spanish Government REMEDIATION (CGL2014-57215-  
391 C4-1-R) and PACE (CGL2017-87216-C4-1-R) projects and the Catalan Government 2017SGR 1733  
392 project. We thank technical support from CCiT-UB and the work of the undergraduate students D.García  
393 and F.Bagaria. D.Rodríguez-Fernández acknowledges FPU2012/01615 and Beca Fundació Pedro i Pons  
394 2014 and M.Rosell, Ramón y Cajal contract (RYC-2012-11920). We thank the editor and the anonymous  
395 reviewers for comments that improved the quality of the manuscript.

## 396 **5. References**

- 397 Adewuyi, Y.G., Carmichael, G.R., 1987. Kinetics of hydrolysis and oxidation of carbon disulfide  
398 by hydrogen peroxide in alkaline medium and application to carbonyl sulfide. *Environ. Sci.*  
399 *Technol.* 21, 170–177. doi:10.1021/es00156a602
- 400 Amonette, J.E., Workman, D.J., Kennedy, D.W., Fruchter, J.S., Gorby, Y.A., 2000.  
401 Dechlorination of carbon tetrachloride by Fe (II) associated with goethite. *Environ. Sci.*  
402 *Technol.* 34, 4606–4613. doi:10.1021/es9913582
- 403 Arnold, W.A., Ball, W.P., Roberts, A.L., 1999. Polychlorinated ethane reaction with zero-valent  
404 zinc: pathways and rate control. *J. Contam. Hydrol.* 40, 183–200. doi:10.1016/S0169-  
405 7722(99)00045-5
- 406 Bonnissel-Gissinger, P., Alnot, M., Ehrhardt, J.J., Behra, P., 1998. Surface oxidation of pyrite as  
407 a function of pH. *Environ. Sci. Technol.* 32, 2839–2845. doi:10.1021/es980213c
- 408 Breider, F., Albers, C.N., Hunkeler, D., 2013. Assessing the role of trichloroacetyl-containing  
409 compounds in the natural formation of chloroform using stable carbon isotopes analysis.  
410 *Chemosphere* 90, 441–448. doi:10.1016/j.chemosphere.2012.07.058
- 411 Burris, D.R., Campbell, T.J., Manoranjan, V.S., 1995. Sorption of trichloroethylene and  
412 tetrachloroethylene in a batch reactive metallic iron-water system. *Environ. Sci. Technol.*  
413 29, 2850–2855. doi:10.1021/es00011a022
- 414 Burris, D.R., Allen-King, R.M., Manoranjan, V.S., Campbell, T.J., Loraine, G.A., Deng, B., 1998.  
415 Chlorinated ethene reduction by cast iron: sorption and mass transfer. *J. Environ. Eng.* 124,  
416 1012–1019. doi:10.1061/(ASCE)0733-9372(1998)124:10(1012)
- 417 Cappelletti, M., Frascari, D., Zannoni, D., Fedi, S., 2012. Microbial degradation of chloroform.  
418 *Appl. Microbiol. Biotechnol.* 96, 1395–1409. doi:10.1007/s00253-012-4494-1
- 419 Choe, S., Lee, S.H., Chang, Y.Y., Hwang, K.Y., Khim, J., 2001. Rapid reductive destruction of  
420 hazardous organic compounds by nanoscale Fe<sup>0</sup>. *Chemosphere* 42, 367–372.  
421 doi:10.1016/S0045-6535(00)00147-8
- 422 Cretnik, S., Thoreson, K.A., Bernstein, A., Ebert, K., Buchner, D., Laskov, C., Haderlein, S.,

- 423 Shouakar-stash, O., Kliegman, S., McNeill, K., Elsner, M., 2013. Reductive dechlorination  
424 of TCE by chemical model systems in comparison to dehalogenating bacteria: Insights from  
425 dual element isotope analysis ( $^{13}\text{C}/^{12}\text{C}$ ,  $^{37}\text{Cl}/^{35}\text{Cl}$ ). *Environ. Sci. Technol.* 47, 6855–6863.  
426 doi:10.1021/es400107n
- 427 Danielsen, K.M., Hayes, K.F., 2004. pH dependence of carbon tetrachloride reductive  
428 dechlorination by magnetite. *Environ. Sci. Technol.* 38, 4745–4752. doi:10.1021/es0496874
- 429 Danielsen, K.M., Gland, J.L., Hayes, K.F., 2005. Influence of amine buffers on carbon  
430 tetrachloride reductive dechlorination by the iron oxide magnetite. *Environ. Sci. Technol.*  
431 39, 756–763. doi:10.1021/es049635e
- 432 Davis, A., Fennimore, G.G., Peck, C., Walker, C.R., McIlwraith, J., Thomas, S., 2003.  
433 Degradation of carbon tetrachloride in a reducing groundwater environment: Implications  
434 for natural attenuation. *Appl. Geochemistry* 18, 503–525. doi:10.1016/S0883-  
435 2927(02)00102-6
- 436 Devlin, J.F., Muller, D., 1999. Field and laboratory studies of carbon tetrachloride transformation  
437 in a sandy aquifer under sulfate reducing conditions. *Environ. Sci. Technol.* 33, 1021–1027.  
438 doi:10.1021/es9806884
- 439 Elsner, M., Haderlein, S.B., Kellerhals, T., Luzi, S., Zwank, L., Angst, W., Schwarzenbach, R.P.,  
440 2004. Mechanisms and products of surface-mediated reductive dehalogenation of carbon  
441 tetrachloride by Fe(II) on goethite. *Environ. Sci. Technol.* 38, 2058–2066.  
442 doi:10.1021/es034741m
- 443 Elsner, M., Zwank, L., Hunkeler, D., Schwarzenbach, R.P., 2005. A new concept linking  
444 observable stable isotope fractionation to transformation pathways of organic pollutants.  
445 *Environ. Sci. Technol.* 39, 6896–6916. doi:10.1021/es0504587
- 446 Elsner, M., Cwiertny, D.M., Roberts, A.L., Sherwood Lollar, B., 2007. 1,1,2,2-Tetrachloroethane  
447 reactions with  $\text{OH}^-$ , Cr(II), granular iron, and a copper - iron bimetal: insights from product  
448 formation and associated carbon isotope fractionation. *Environ. Sci. Technol.* 41, 4111–  
449 4117. doi:10.1021/es072046z
- 450 Elsner, M., 2010. Stable isotope fractionation to investigate natural transformation mechanisms  
451 of organic contaminants: principles, prospects and limitations. *J. Environ. Monit.* 12, 2005–  
452 2031. doi:10.1039/c0em00277a
- 453 Farrell, J., Kason, M., Melitas, N., Li, T., 2000. Investigation of the long-term performance of  
454 zero-valent iron for reductive dechlorination of trichloroethylene. *Environ. Sci. Technol.* 34,  
455 514–521. doi:10.1021/es990716y
- 456 Feng, J., Lim, T.T., 2005. Pathways and kinetics of carbon tetrachloride and chloroform  
457 reductions by nano-scale Fe and Fe/Ni particles: Comparison with commercial micro-scale  
458 Fe and Zn. *Chemosphere* 59, 1267–1277. doi:10.1016/j.chemosphere.2004.11.038
- 459 Feng, J., Zhu, B.-W., Lim, T.T., 2008. Reduction of chlorinated methanes with nano-scale Fe  
460 particles: Effects of amphiphiles on the dechlorination reaction and two-parameter  
461 regression for kinetic prediction. *Chemosphere* 73, 1817–1823.  
462 doi:10.1016/j.chemosphere.2008.08.014
- 463 Ferrey, M.L., Wilkin, R.T., Ford, R.G., Wilson, J.T., 2004. Nonbiological removal of cis-  
464 dichloroethylene and 1,1-dichloroethylene in aquifer sediment containing magnetite.  
465 *Environ. Sci. Technol.* 38, 1746–1752. doi:10.1021/es0305609
- 466 Hanoch, R.J., Shao, H., Butler, E.C., 2006. Transformation of carbon tetrachloride by bisulfide  
467 treated goethite, hematite, magnetite, and kaolinite. *Chemosphere* 63, 323–334.  
468 doi:10.1016/j.chemosphere.2005.07.016
- 469 He, Y.T., Wilson, J.T., Su, C., Wilkin, R.T., 2015. Review of abiotic degradation of chlorinated  
470 solvents by reactive iron minerals in aquifers. *Groundw. Monit. Remediat.* 35, 57–75.  
471 doi:10.1111/gwmr.12111
- 472 Heckel, B., Cretnik, S., Kliegman, S., Shouakar-Stash, O., McNeill, K., Elsner, M., 2017a.  
473 Reductive outer-sphere single electron transfer is an exception rather than the rule in natural  
474 and engineered chlorinated ethene dehalogenation. *Environ. Sci. Technol.* 51, 9663–9673.  
475 doi:10.1021/acs.est.7b01447
- 476 Heckel, B., Rodríguez-Fernández, D., Torrentó, C., Meyer, A., Palau, J., Domènech, C., Rosell,  
477 M., Soler, A., Hunkeler, D., Elsner, M., 2017b. Compound-specific chlorine isotope analysis

478 of tetrachloromethane and trichloromethane by gas chromatography-isotope ratio mass  
479 spectrometry vs gas chromatography-quadrupole mass spectrometry: method development  
480 and evaluation of precision and trueness. *Anal. Chem.* 89, 3411–3420.  
481 doi:10.1021/acs.analchem.6b04129

482 Helland, B.R., Alvarez, P.J.J., Schnoor, J.L., 1995. Reductive dechlorination of carbon  
483 tetrachloride with elemental iron. *J. Hazard. Mater.* 41, 205–216. doi:10.1016/0304-  
484 3894(94)00111-S

485 Hosono, T., Nakano, T., Shimizu, Y., Onodera, S. ichi, Taniguchi, M., 2011. Hydrogeological  
486 constraint on nitrate and arsenic contamination in Asian metropolitan groundwater. *Hydrol.*  
487 *Process.* 25, 2742–2754. doi:10.1002/hyp.8015

488 Huang, K.C., Zhao, Z., Hoag, G.E., Dahmani, A., Block, P.A., 2005. Degradation of volatile  
489 organic compounds with thermally activated persulfate oxidation. *Chemosphere* 61, 551–  
490 560. doi:10.1016/j.chemosphere.2005.02.032

491 Huling, S.G., Pivetz, B.E., 2006. In-Situ Chemical Oxidation-Engineering issue. EPA/600/R-  
492 06/072. U.S. Environmental Protection Agency Office of Research and Development,  
493 National Risk Management Research Laboratory: Cincinnati, OH.

494 Hunkeler, D., Laier, T., Breider, F., Jacobsen, O.S., 2012. Demonstrating a natural origin of  
495 chloroform in groundwater using stable carbon isotopes. *Environ. Sci. Technol.* 46, 6096–  
496 6101. doi:10.1021/es204585d

497 IARC, 1999. IARC Monographs on the evaluation of carcinogenic risks to humans 71, 319–335.

498 Jeffers, P.M., Ward, L.M., Woytowlitch, L.M., Wolfe, N.L., 1989. Homogeneous hydrolysis rate  
499 constants for selected chlorinated methanes, ethanes, ethenes, and propanes. *Environ. Sci.*  
500 *Technol.* 23, 965–969. doi:10.1021/es00066a006

501 Kim, Y.H., Carraway, E.R., 2000. Dechlorination of pentachlorophenol by zero valent iron and  
502 modified zero valent irons. *Environ. Sci. Technol.* 34, 2014–2017. doi:10.1021/es991129f

503 Koenig, J., Lee, M., Manefield, M., 2015. Aliphatic organochlorine degradation in subsurface  
504 environments. *Rev. Environ. Sci. Bio/Technology* 14, 49–71. doi:10.1007/s11157-014-  
505 9345-3

506 Kriegman-King, M.R., Reinhard, M., 1992. Transformation of carbon tetrachloride in the  
507 presence of sulfide, biotite, and vermiculite. *Environ. Sci. Technol.* 26, 2198–2206.  
508 doi:10.1021/es00035a019

509 Kriegman-King, M.R., Reinhard, M., 1994. Transformation of carbon tetrachloride by pyrite in  
510 aqueous solution. *Environ. Sci. Technol.* 28, 692–700. doi:10.1021/es00053a025

511 Lee, M., Wells, E., Wong, Y.K., Koenig, J., Adrian, L., Richnow, H.H., Manefield, M., 2015.  
512 Relative contributions of *Dehalobacter* and zerovalent iron in the degradation of chlorinated  
513 methanes. *Environ. Sci. Technol.* 49, 4481–4489. doi:10.1021/es5052364

514 Lien, H.L., Zhang, W.X., 1999. Transformation of chlorinated methanes by nanoscale iron  
515 particles. *J. Environ. Eng.* 125, 1042–1047. doi:10.1061/(ASCE)0733-  
516 9372(1999)125:11(1042)

517 Lien, H.-L., Jhuo, Y.-S., Chen, L.-H., 2007. Effect of heavy metals on dechlorination of carbon  
518 tetrachloride by iron nanoparticles. *Environ. Eng. Sci.* 24, 21–30.  
519 doi:10.1089/ees.2007.24.21

520 Maithreepala, R.A., Doong, R., 2007. Dechlorination of carbon tetrachloride by ferrous ion  
521 associated with iron oxide nano particles, in: *Proceedings of the Fourth Academic Sessions*  
522 *2007.*

523 Martín-González, L., Mortan, S.H., Rosell, M., Parladé, E., Martínez-Alonso, M., Gaju, N.,  
524 Caminal, G., Adrian, L., Marco-Urrea, E., 2015. Stable carbon isotope fractionation during  
525 1,2-dichloropropane-to-propene transformation by an enrichment culture containing  
526 *Dehalogenimonas* strains and a *dcpA* gene. *Environ. Sci. Technol.* 49, 8666–8674.  
527 doi:10.1021/acs.est.5b00929

528 Matheson, L.J., Tratnyek, P.G., 1994. Reductive dehalogenation of chlorinated methanes by iron  
529 metal. *Environ. Sci. Technol.* 28, 2045–2053. doi:10.1021/es00061a012

530 McGeough, K.L., Kalin, R.M., Myles, P., 2007. Carbon disulfide removal by zero valent iron.  
531 *Environ. Sci. Technol.* 41, 4607–4612. doi:http://dx.doi.org/10.1021/es062936z

532 Morris, B.L., Lawrence, A.R.L., Chilton, P.J.C., Adams, B., C, C.R., Klinck, B.A., 2003.

533 Groundwater and its susceptibility to degradation: a global assessment of the problem and  
534 options for management. Early Warning and Assessment Report Series, RS. 03-3., United  
535 Nations Environment Programme. Nairobi, Kenya. doi:10.1017/CBO9781107415324.004

536 Nijenhuis, I., Renpenning, J., Kümmel, S., Richnow, H.H., Gehre, M., 2016. Recent advances in  
537 multi-element compound-specific stable isotope analysis of organohalides: Achievements,  
538 challenges and prospects for assessing environmental sources and transformation. Trends  
539 Environ. Anal. Chem. 11, 1–8. doi:10.1016/j.teac.2016.04.001

540 Obiri-Nyarko, F., Grajales-Mesa, S.J., Malina, G., 2014. An overview of permeable reactive  
541 barriers for in situ sustainable groundwater remediation. Chemosphere 111, 243–259.  
542 doi:10.1016/j.chemosphere.2014.03.112

543 Palau, J., Marchesi, M., Chambon, J.C.C., Aravena, R., Canals, À., Binning, P.J., Bjerg, P.L.,  
544 Otero, N., Soler, A., 2014. Multi-isotope (carbon and chlorine) analysis for fingerprinting  
545 and site characterization at a fractured bedrock aquifer contaminated by chlorinated  
546 ethenes. Sci. Total Environ. 475, 61–70. doi:10.1016/j.scitotenv.2013.12.059

547 Pecher, K., Haderlein, S.B., Schwarzenbach, R.P., 2002. Reduction of polyhalogenated methanes  
548 by surface-bound Fe(II) in aqueous suspensions of iron oxides. Environ. Sci. Technol. 36,  
549 1734–1741. doi:10.1021/es011191o

550 Penny, C., Vuilleumier, S., Bringel, F., 2010. Microbial degradation of tetrachloromethane:  
551 mechanisms and perspectives for bioremediation. FEMS Microbiol. Ecol. 74, 257–275.  
552 doi:10.1111/j.1574-6941.2010.00935.x

553 Peyton, T.O., Steel, R. V., Mabey, W.R., 1976. Carbon disulfide, carbonyl sulfide: literature  
554 review and environmental assessment (EPA-600/9-78-009). Washington, DC.

555 Renpenning, J., Nijenhuis, I., 2016. Evaluation of the microbial reductive dehalogenation reaction  
556 using Compound-Specific Stable Isotope Analysis (CSIA), in: Adrian, L., Löffler, E.F.  
557 (Eds.), Organohalide-Respiring Bacteria. Springer Berlin Heidelberg, Berlin, pp. 429–453.  
558 doi:10.1007/978-3-662-49875-0\_18

559 Rodríguez-Fernández, D., Torrentó, C., Guivernau, M., Viñas, M., Hunkeler, D., Soler, A.,  
560 Domènech, C., Rosell, M., 2018. Vitamin B<sub>12</sub> effects on chlorinated methanes-degrading  
561 microcosms: dual isotope and metabolically active microbial populations assessment. Sci.  
562 Total Environ. 621, 1615–1625. doi:10.1016/j.scitotenv.2017.10.067

563 Scherer, M.M., Balko, B.A., Tratnyek, P.G., 1998. The role of oxides in reduction reactions at the  
564 metal-water interface, in: T. G. (Ed.), Kinetics and Mechanisms of Reactions at the  
565 Mineral/water Interface, ACS Symposium Series, Division of Geochemistry. Washington,  
566 DC, pp. 301–322.

567 Scheutz, C., Durant, N.D., Hansen, M.H., Bjerg, P.L., 2011. Natural and enhanced anaerobic  
568 degradation of 1,1,1-trichloroethane and its degradation products in the subsurface - A  
569 critical review. Water Res. 45, 2701–2723. doi:10.1016/j.watres.2011.02.027

570 Song, H., Carraway, E.R., 2006. Reduction of chlorinated methanes by nano-sized zero-valent  
571 iron. Kinetics, pathways and effect of reaction conditions. Environ. Eng. Sci. 23, 272–284.  
572 doi:10.1089/ees.2006.23.272

573 Svoronos, P.D.N., Bruno, T.J., 2002. Carbonyl Sulfide: A review of its chemistry and properties.  
574 Ind. Eng. Chem. Res. 41, 5321–5336. doi:10.1021/ie020365n

575 Támara, M.L., Butler, E.C., 2004. Effects of iron purity and groundwater characteristics on rates  
576 and products in the degradation of carbon tetrachloride by iron metal. Environ. Sci. Technol.  
577 38, 1866–1876. doi:10.1021/es0305508

578 Thullner, M., Centler, F., Richnow, H.H., Fischer, A., 2012. Quantification of organic pollutant  
579 degradation in contaminated aquifers using compound specific stable isotope analysis -  
580 Review of recent developments. Org. Geochem. 42, 1440–1460.  
581 doi:10.1016/j.orggeochem.2011.10.011

582 Thullner, M., Fischer, A., Richnow, H.-H., Wick, L.Y., 2013. Influence of mass transfer on stable  
583 isotope fractionation. Appl. Microbiol. Biotechnol. 97, 441–452. doi:10.1007/s00253-012-  
584 4537-7

585 Torrentó, C., Audí-Miró, C., Bordeleau, G., Marchesi, M., Rosell, M., Otero, N., Soler, A., 2014.  
586 The use of alkaline hydrolysis as a novel strategy for chloroform remediation: The feasibility  
587 of using construction wastes and evaluation of carbon isotopic fractionation. Environ. Sci.

588 Technol. 48, 1869–1877. doi:10.1021/es403838t  
589 Torrentó, C., Palau, J., Rodríguez-Fernández, D., Heckel, B., Meyer, A., Domènech, C., Rosell,  
590 M., Soler, A., Elsner, M., Hunkeler, D., 2017. Carbon and chlorine isotope fractionation  
591 patterns associated with different engineered chloroform transformation reactions. Environ.  
592 Sci. Technol. 51, 6174–6184. doi:10.1021/acs.est.7b00679  
593 Van Breukelen, B.M., 2007. Extending the Rayleigh equation to allow competing isotope  
594 fractionating pathways to improve quantification of biodegradation. Environ. Sci. Technol.  
595 41, 4004–4010. doi:10.1021/es0628452  
596 Vikesland, P.J., Heathcock, A.M., Rebodos, R.L., Makus, K.E., 2007. Particle size and  
597 aggregation effects on magnetite reactivity toward carbon tetrachloride. Environ. Sci.  
598 Technol. 41, 5277–5283. doi:10.1021/es062082i  
599 Vodyanitskii, Y.N., 2014. Effect of reduced iron on the degradation of chlorinated hydrocarbons  
600 in contaminated soil and ground water: A review of publications. Eurasian Soil Sci. 47, 119–  
601 133. doi:10.1134/S1064229314020136  
602 Zogorski, J.S., Carter, J.M., Ivahnenko, T., Lapham, W.W., Moran, M.J., Rowe, B.L., Squillace,  
603 P.J., Toccalino, P.L., 2006. The quality of our nation's waters - Volatile organic compounds  
604 in the nation's groundwater and drinking-water supply wells, U.S. Geological Survey  
605 Circular 1292.  
606 Zwank, L., Elsner, M., Aeberhard, A., Schwarzenbach, R.P., 2005. Carbon isotope fractionation  
607 in the reductive dehalogenation of carbon tetrachloride at iron (hydr)oxide and iron sulfide  
608 minerals. Environ. Sci. Technol. 39, 5634–5641. doi:10.1021/es0487776